Wavelet-based deconvolution in non destructive evaluation

R H Herrera[1], E. Moreno[2] and R. Orozco[3]

[1]University of Cienfuegos, Cienfuegos, Cuba
[2]Institute of Cibernetics, Mathematics and Physics, Havana, Cuba
[3]University of Las Villas, Santa Clara, Cuba

E-mail: henry@finf.ucf.edu.cu, moreno@icmf.inf.cu, rorozco@fie.uclv.edu.cu

Abstract. The problem of substraction the medium response to an ultrasonic pulse from the measure signal blurred by the structural and system noise has been treated in this work. This ill-conditioned problem is solved by wavelet-based blind deconvolution, then the propose algorithm becomes robust for processing the radiofrequency (RF) A-scan signals as initial steps for SAFT image reconstruction. The results shows an improved axial resolution quantified through the main lobe of the covariance function.

Submitted to: *Inverse Problems*

1. Introduction

Deconvolution of ultrasonic signals is defined as the solution of the inverse problem of extracting the medium reflectivity function from the blurring effects of the transducer pulse and can be represented by [1]:

$$y(n) = x(n) * h(n) + \eta(n) \tag{1}$$

where *y(n)* is the measured signal, $*$ denotes the convolution operation, $h(n)$ is the temporal extension of the pulse or simply the ultrasound pulse and *η(n)* is an independent noise term that always has to be added for real systems [2]. To recover *x(n)* from the observation *y(n)* drives to improve the appearance and the axial resolution of the images through the elimination of the dependent effects of the measuring system [1]. The signal *y(n)* corresponds to A-scan lines of 2-D acoustic image or 1-D signal, where the problem settles down by taking the desired signal *x(n)* as the input of a linear time invariant system (LTI) with impulse response *h(n)* [1]. The output of the LTI system is blurred by white Gaussian noise *η(n)* of variance σ_η^2. In the frequency domain from (1) we get:

$$Y(f) = H(f)X(f) + N(f) \tag{2}$$

where: *Y(f)*, *H(f)* and *N(f)* are the Fourier transform of *y(n)*, *h(n)* and $\eta(n)$ respectively. Inverse filtering can be applied to (2):

$$X_1(f) = H^{-1}(f)Y(f) = X(f) + H^{-1}(f)N(f) \tag{3}$$

But this holds only if the system frequency response *H(f)* is invertible. However where *H(f)* takes near to zero values, the noise is highly amplified with variance spreading to infinite which leads to incorrect estimates. In this case it is necessary to include in the inverse filter some regularization parameter which reduces the variance of the estimated signal. The most known case of regularized filter for stationary signals is the Wiener filter [3]. When the signals under analysis shows non stationary properties, as abrupt changes, the Wiener filter based on the Fourier transform does not give satisfactory results in the estimation, conditioned by the characteristics of Fourier basis of complex exponentials. It is known that wavelets orthonormal basis achieves a better matching with the transmitted pulse and drives to a better localization in time and frequency [3]. Another of the advantages of wavelets is that the signals can be represented with some few coefficients different from zero, which corresponds with the ultrasonic signals, where the trace is only composed by values different from zero in cases of abrupt changes of acoustic impedance. This leads to an efficient methods of compression and noise filtering.

R. Neelamani et. al., recently proposed a wavelet-based regularized deconvolution technique (ForWaRD) [4], which will be used in this paper for the deconvolution of ultrasonic signals as a first step to the reconstruction of acoustic images by means of Synthetic Aperture Focusing Testing (SAFT).

The initial problem in deconvolution, is the a priori knowledge or not of the system impulse response *h(n)*. Oppenhiem and Schafer have defined the case of estimating *x(n)* from *h(n)* as the well-known homomorphic deconvolution [5], using the real cepstrum for minimum phase signals or the complex cepstrum for the most general case. T. Taxt in [2], compares seven methods based on the cepstrum for blind deconvolution in the estimation of the reflectivity function in biological media. Michailovich and Adam in [6] has proposed a wavelet-based projection method (WBPM) where the estimate is obtained as a projection of the RF-line log-spectrum onto the subspace spanned by predefined wavelets functions. But in all this methods some previous knowledge of the system is required or the assumption of minimal-phase pulse most be considered, something that depends on the construction of the housing of the pieso-electric and of the impedance matching between the transmitter and the crystal [6].

We select the method of Higher Order Spectral Analysis (HOSA) because of its immunity to noise and the not initial conditionality that the transducer's electromechanical impulse response is of minimum phase [1]. The process is divided into two stages: the first is the estimation of the ultrasound pulse from the bicepstrum. Once an estimated of this function is obtained, it is used to cancel out the blurring effect of the pulse from the observation data by the selected deconvolution procedure. The second stage is the reconstruction of the SAFT image from the deconvolved RF-lines.

2. Pulse estimation using higher order spectral analysis

This Section firstly describes the method used for estimating the system function and continues with the wavelet-based deconvolution.

The system function described in (1) as the transducer's impulse response *h(n)* is a deterministic and causal FIR filter, *x(n)* represents the medium response function that we assume initially, without a loss of generality, stationary, zero mean and non Gaussian distribution. This last property guarantees that its third-order cumulant exists, and $\eta(n)$ represents the zero mean Gaussian noise that is uncorrelated with *x(n)*. The third-order cumulant of the zero mean signal *y(n)* is represented by [7, **?**]:

$$c_3^y(m_1, m_2) = \gamma_3^x \frac{1}{M} \sum_{k=0}^{M-1} h(k)h(k+m_1)h(k+m_2) \tag{4}$$

where $\gamma_3^x = E[x^3(n)]$, is a constant equal to the third cumulant of the signal *x(n)*, and $E[\cdot]$ is the operator of statistical average.

The Gaussian condition of the noise $\eta(n)$ was assumed in (4), therefore its third order cumulant $c_3^\eta = 0$. By applying the 2-D Z-transform (Z_2) to (4) we get the bispectrum:

$$C_3^y(z_1, z_2) = \gamma_3^x H(z_1)H(z_2)H(z_1^{-1}z_2^{-1}) \tag{5}$$

The bicepstrum $b_y(m_1, m_2)$, is obtained as was described in [**?**], logarithm of the bispectrum and inverse transformation to arrive into the 2-D quefrency domain:

$$b_y(m_1, m_2) = Z_2^{-1}[log(C_3^y(z_1, z_2))] \tag{6}$$

where Z_2^{-1} is the bidimensional inverse Z transform. Instead of (6) we use the *FFT* based bicepstrum method proposed by Pan and Nikias [8] for the signal reconstruction problem due to the long support of the cepstrum. The bicepstrum is achieved by:

$$b_y(m_1, m_2) = F_2^{-1}\left\{\frac{F_2[m_1 c_3^y(m_1, m_2)]}{F_2[c_3^y(m_1, m_2)]}\right\} \tag{7}$$

where F_2 and F_2^{-1}, denotes the direct and inverse 2-D Fourier transform respectively. The cepstrum $\hat{h}(n)$ of $h(n)$ is then retrieved along the diagonal $m_1 = m_2$ for all $n \neq 0$ in the bicepstrum domain.

The bicepstrum is defined as the cepstrum of the biespectrum [7] then in the transformed domain:

$$b_y(m_1, m_2) = b_x(m_1, m_2) + b_h(m_1, m_2) \tag{8}$$

where $b_x(m_1, m_2)$ is the bicepstrum of $x(n)$ and $b_h(m_1, m_2)$ is the corresponding bicepstrum of $h(n)$. As has been shown by Abeyratne et. al. [7], if $x(n)$ is stationary independent identically distribuited (i.i.d), its thrid-order spectrum is flat and equal to the skewness γ_3^x, and its bicepstrum is an impulse located at the origin. The bicepstral values along the main axes ($m_1 = 0$, $m_2 = 0$) and the diagonal $m_1 = m_2$ are nonzero. The complex cepstrum $\hat{h}(n)$ is obtained by evaluating the bicepstral values along the

lines $b_x(m_1, 0)$ or $b_x(0, m_2)$ or in the main diagonal $m_1 = m_2$ except at the origin $m_1 = m_2 = 0$. The inverse relation is as follows:

$$\hat{h}(n) = b_y(-n, -n) \qquad n \neq 0 \tag{9}$$

The reconstructed version can be obtained by:

$$h(n) = F^{-1}\{e^{F(\hat{h}(n)}\} \tag{10}$$

where F and F^{-1} are the direct and inverse Fourier transform respectively.

The value $\hat{h}(0)$ cannot be determined as γ_3^x is unknown, but its exact value is not needed as a different $\hat{h}(0)$ only results in a different scaled version of the pulse $h(n)$ [1].

The main advantage of this estimation method is that the bispectrum of the white Gaussian noise is zero [6], which allows us to estimate $h(n)$ without taking into account the contribution of $\eta(n)$ in (1).

Once the pulse has been estimated the reflectivity function can be obtained by a deconvolution process.

3. The Wiener Filter

Having $h(n)$ we can estimate $X_1(f)$ using a simple Wiener filter [9, 2]:

$$X_1(f) = Y(f)\left[\frac{H^*(f)}{|H(f)|^2 + q}\right] \tag{11}$$

Where q is a term that includes the regularization parameter and the noise contribution, $H(f)$ is the 1-D Fourier transform of $h(n)$ and its complex conjugated. The parameter q has been assumed as the square noise-to-signal ratio and is measured directly from the recorded radio frequency data (see [2]). The term inside the brackets in (11) is the inverse Wiener filter. In generic form is represented by [1]:

$$G(f) = \frac{H^*(f)P_{x_1}(f)}{|H(f)|^2 P_{x_1}(f) + \alpha\sigma_n^2} \tag{12}$$

where $P_{x_1}(f)$, is the power spectral density of $x_1(n)$, α is the regularization parameter and σ_n^2 represents the noise variance. As $P_{x_1}(f)$ is unknown it is necessary to use the iterative Wiener method, in this study we took $\alpha = 0.01$ initially, giving good results in the estimate and σ_n^2 was calculated as the median of the finest scale wavelets coefficients of $y(n)$ [10], $x_1(n)$ is obtained from $X_1(f)$ by inverse Fourier transformation.

3.1. Wavelet-Based Wiener Filter

The discrete wavelet transform (DWT) represents a $1 - D$ continuous-time signal $x(t)$, in terms of shifted versions of a lowpass scaling function ϕ and shifted and dilated versions of a prototype band-pass wavelet function ψ [4]. As it was demonstrated by I. Daubechies [**?**], special cases of these functions and form an orthonormal basis in the space, with . The parameter j is associated with the scale of the analysis and k with

the localization or displacement. Signal decomposition at a level J, would be given by [1]:

$$x^J(t) = \sum_{k=1}^{2^{N-J}} c(k)\phi_k(t) + \sum_{j=1}^{J}\sum_{k=1}^{2^{N-J}} d(j,k)\psi_{j,k}(t) \tag{13}$$

where $c(k)$ is the inner product $c(k) = \langle x(t), \phi_{j,k}(t)\rangle$ and $c(k) = \langle x(t), \psi_{j,k}(t)\rangle$ The estimated signal from the Wiener filter is projected into this base, and at each decomposition level the variance σ_j^2 is obtained for noise reduction. The following step is to use the Wiener filter in the wavelet domain where the filtering process is done for the wavelet coefficients. From (10) we have [4]:

$$\lambda_{j,k}^d = \frac{|d_{j,k}|^2}{|d_{j,k}|^2 + \sigma_j^2}, \quad and \quad \lambda_{j,k}^c = \frac{|c_{j,k}|^2}{|c_{j,k}|^2 + \sigma_j^2}, \tag{14}$$

By substituting (11) in (10) we obtain the expression of the estimated reflectivity function $\tilde{x}(n)$:

$$\tilde{x}(n) = \sum_{k=1}^{2^{N-J}} \lambda_{j,k}^c c(k)\phi_k(t) + \sum_{j=1}^{J}\sum_{k=1}^{2^{N-J}} \lambda_{j,k}^d d_{j,k}\psi_{j,k}(t) \tag{15}$$

3.2. Experimental Setup

The experimental system consisted on the obtaining an acoustic image of 10 bars of acrylic of diameter 5 mm, submerged in water. A data set of 400 RF-sequences has been generated, each RF-sequence containing 9995 sampling points. The RF-lines were sampled at a rate of 50 MHz. An unfocused 3.5 MHz transducer was used in both emission and reception operating in pulse-echo mounted in a scanner controlled by stepping motor with 0.20mm between A-scan lines.

4. Results and Discussion

The deconvolution process steps, as has been described previously include:

(i) Estimate the impulse response from the bicepstrum.

(ii) Obtain a first estimate of the reflectivity function using the regularized Wiener filter in the domain of the frequency.

(iii) Apply a noise filtering over the wavelets coefficients.

(iv) Estimate the reflectivity function with the Wiener filter in the wavelet domain.

4.1. Estimation of the Ultrasound Pulse

The pulse estimation was carried out on a set of 16 zero mean signals. Fig. 1 shows the obtained pulse, using the MatLab function bicepsf.m of the HOSA Toolbox.

The spectral content of the obtained pulse includes the same band of the original signal.

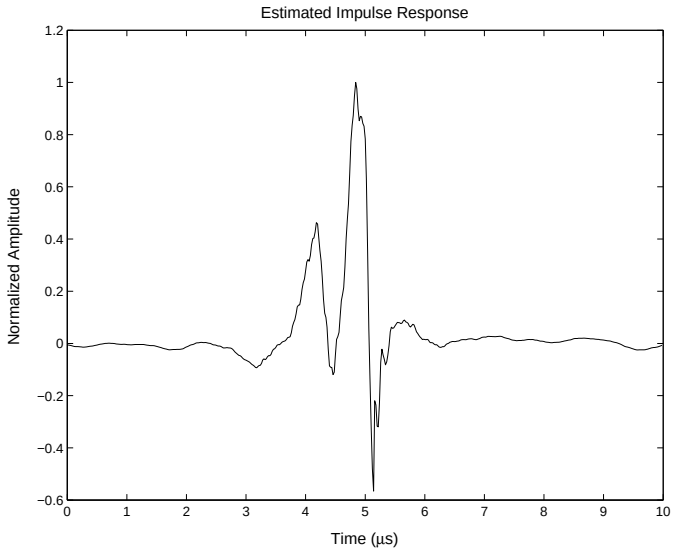

Figure 1. Estimated impulse response. The normalized pulse width vs time in μs

4.2. Estimation of the reflectivity function

We used an iterative Wiener filter to estimate the power spectral density $Px_1(f)$, as was explained in the section 2.2. After ten iterations the signal $x_1(n)$ was obtained. Fig. 2 shows a segment of the original signal and the estimated one.

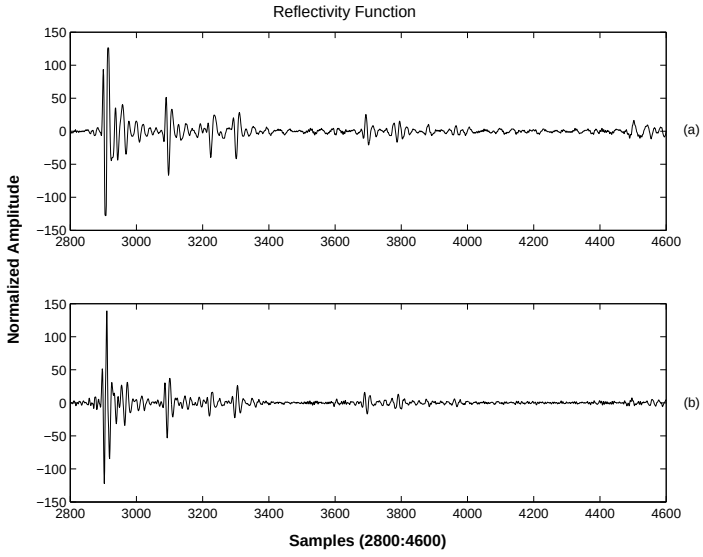

Figure 2. Estimated reflectivity function obtained by iterative Wiener filter. (upper plot) The original signal $y(n)$; (lower plot) the estimated signal $x_1(n)$

4.3. Noise Filtering

We used a soft threshold over the wavelets coefficients after a decomposition using DB16 and DB10 in the algorithm proposed in [4]. Fig. 3 shows the result of the deconvolution in the wavelet domain. The estimated signal shows a better spatial localization, which improves the axial resolution. In accordance with Fig. 4, the deconvolution of the RF signal improves the resolu-tion, quantified as the decrease of the main lobe width of the autocovariance function [6]. The lobe width at half amplitude (-6dB drop) given in samples is 9 samples for the original signal and 4 for estimated one.

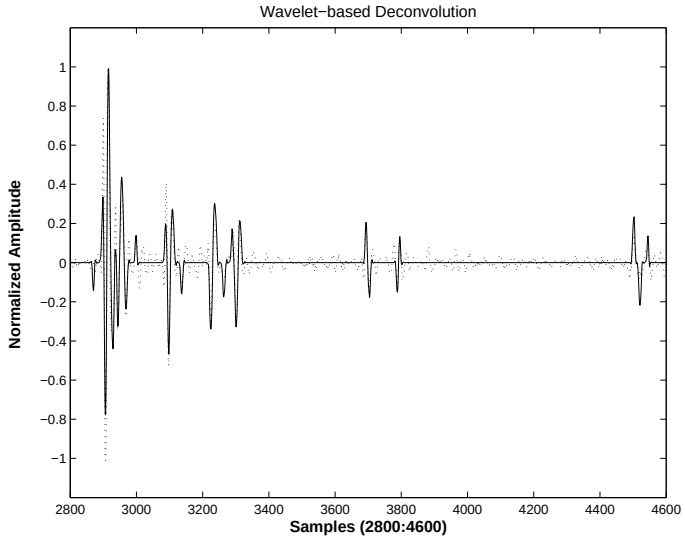

Figure 3. The Wiener filter applied to the wavelets coefficients. (upper plot) The original signal $y(n)$; (lower plot) the deconvolved signal $\tilde{x}(n)$

We obtained an increment of the axial resolution in a factor of 2.25. The same procedure was applied to the set of 30 signals of a total of 400 to characterize the standard deviation of the values, obtaining a factor of 2.25 0.36. This increment of the axial resolution depends of the transducer's spectral proper-ties; consequently it is suggested to prove the method with different frequency band-width ratio.

5. Conclusions

This paper establishes a cepstrum-based method using high-order statistics as the first step for the blind deconvolution kernel estimation which is used in the inverse filter design in both Fourier and wavelet domain for the reconstruction of the medium reflectivity function. This procedure results in a significant reduction of the time spatial support, suggesting a significant gain in the axial resolution. This property is particularly useful in the case of acoustic image generation, where we will apply these results.

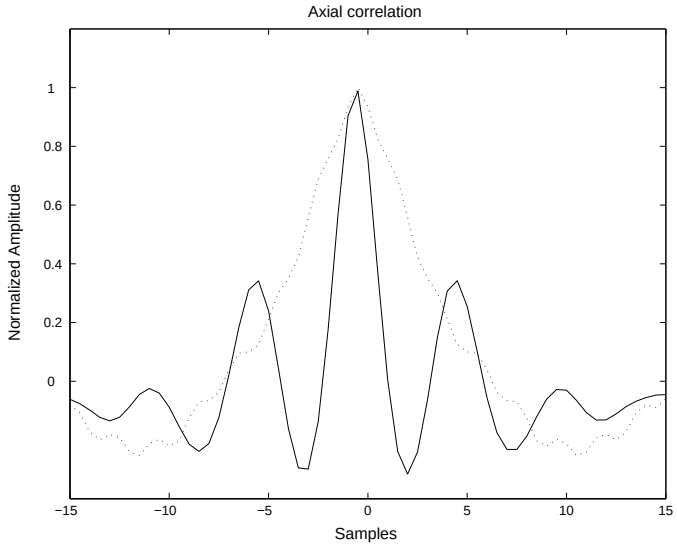

Figure 4. Autocovariance function of the original signal (dotted line) and of the estimated signal (continuous line). The amplitude was normalized in both functions and centered in their maximum

Acknowledgments

Thanks to Mr. R. Copa for reviewing the material and his useful suggestions.

References

[1] Wan S, Raju B I and Srinivasan M A 2003 *IEEE Trans. Ultrason., Ferroelect., Freq. Contr.* **50**(10) 1286–1295
[2] Taxt T 1997 *IEEE Trans. Ultrason., Ferroelect., Freq. Contr.* **44**(3) 666–674
[3] *N*eelamani R, Choi H and Baraniuk R 1999 *IEEE Conf. Acoust. Speech, and Signal Processing (ICAASP)* **6** 3241–3244 http://www-dsp.rice.edu/publications/pub/neelsh98icassp.pdf
[4] *N*eelamani R, Choi H and Baraniuk R 2004 *IEEE Trans. Ultrason., Ferroelect., Freq. Contr.* **52**(2) 418–432
[5] Oppenhiem A V and Schafer R W 1989 *Discrete-Time Signal Procesing* (Prentice-Hall)
[6] Adam D and Michailovich O 2002 *IEEE Trans. Biomedical Eng.* **49**(2) 118–131
[7] Aberyratne U R, Petropulu A P and Reid J M 1995 *IEEE Trans. Ultrason., Ferroelect., Freq. Contr.* **42**(6) 1064–1075
[8] Pan R and Nikias C L 1988 *IEEE Trans. ASSP* **36**(2) 186–205
[9] Honarvar F, Sheikhzadeh H, Moles M and Sinclair A N 2004 *Ultrasonics* **41** 755–763
[10] Donoho D L 1995 *IEEE Trans. Inform., Theory* pp 613–627